

Optimization of fluorinated interfacial layers with minimal surface coverage for hybrid perovskite materials

Riva Alkarsifi,^{†§} Thierry Buffeteau,[†] Christine Labrugère-Sarroste,[‡] Lionel Hirsch,[§] Dario M. Bassani^{†*} and Thierry Toupance^{†*}

[†] Univ. Bordeaux, CNRS, Bordeaux INP, ISM, UMR 5255, F-33400 Talence, France

[‡] Univ. Bordeaux, CNRS, PLACAMAT, UAR 3626, F-33600 Pessac, France

[§] Univ. Bordeaux, IMS, CNRS, UMR 5218, Bordeaux INP, ENSCBP, F-33400 Talence, France

Materials and chemicals

All reactions were carried out under a nitrogen atmosphere. All reagent-grade chemicals were obtained from commercial suppliers and were used as received unless otherwise stated. Anhydrous dimethylformamide (DMF), Toluene, and α,α,α -trifluorotoluene were purchased from Merck and used as received. Analytical thin layer chromatography was performed using silica gel 60 F254 pre-coated plates (Merck) with visualization by potassium permanganate. Column chromatography was performed on silica gel (0.043-0.063 mm).

Characterization

Solution ¹H NMR, ¹³C NMR, ¹⁹F and ¹¹⁹Sn NMR spectra were recorded on Bruker Avance I 300 MHz and Avance III 600 MHz spectrometers at CESAMO (Bordeaux University). Chemical shift values are reported in ppm with reference to solvent residual signals. Mass spectra were also

performed by CESAMO (Bordeaux, France) on a Qexactive mass spectrometer (Thermo). The instrument is equipped with an electrospray (ESI) source and spectra were recorded in the negative mode. The spray voltage was maintained at 3200 V and capillary temperature set at 320°C. Samples were introduced by injection through a 20 μ L sample loop into a 300 μ L/min flow of methanol from the LC pump. MALDI-MS spectra were performed as well by CESAMO (Bordeaux, France) on an Autoflex maX TOF mass spectrometer (Bruker Daltonics, Bremen, Germany) equipped with a frequency tripled Nd:YAG laser emitting at 355 nm. Spectra were recorded in the positive-ion mode using the reflectron and with an accelerating voltage of 19 kV. The acquisition was made in LDI mode. Samples were dissolved in chloroform at 10 mg/mL. One to two microliters of the obtained solution were deposited onto the sample target and vacuum-dried.

SYNTHESIS

Synthesis of $(C_6F_{13}C_2H_4)_4Sn$ (**1b**). This was prepared as mentioned in the literature with some modifications.¹ A Grignard reagent was prepared by stirring a mixture of magnesium turnings (30 mmol, 0.73 g) in dry Et_2O (30 mL) for 1 h at ambient temperature and under nitrogen. A solution of $C_6F_{13}C_2H_4I$ (11.85 g, 25 mmol) in dry Et_2O (30 mL) with two drops of 1,2-dibromoethane was slowly added at 0°C. The reaction mixture was stirred for 3 h at this temperature before dry Et_2O (30 mL) was added. $SnCl_4$ (1.3 g, 5 mmol) dissolved in dry toluene (20 mL) was added dropwise, after which the mixture was heated under reflux for 4 days. The reaction was hydrolyzed by the slow addition of water (30 mL), and the mixture was filtered through Celite and then washed with pentane. The filtrates were extracted with ethyl acetate. The organic phase was washed twice with water, dried over $MgSO_4$, and concentrated by rotary evaporation. The crude product was finally

purified by the classical column chromatography on silica gel using hexane as an eluent to give **1b** (40% yield) as a colorless oil.

^1H NMR (300.2 MHz, CDCl_3) δ 1.13 (t, 8H, $^3J_{\text{H-H}} = 8$ Hz, $^2J_{\text{Sn-H}} = 52$ Hz), 2.29 (tt, 8H, $^3J_{\text{F-H}} = 18$ Hz, $^3J_{\text{H-H}} = 8$ Hz); ^{19}F NMR (282.4 MHz, CDCl_3) δ - 80.94 (t, 12F), -116.71 (m, 8F), -122.01 (m, 8F), -122.98 (m, 8F), -123.68 (m, 8F), -126.27 (m, 8F); ^{13}C NMR (75 MHz, CDCl_3) δ -1.67 (s, C-Sn), 27.44 (t, $^2J_{\text{C-F}} = 23$ Hz); ^{119}Sn NMR (223.8 MHz, CDCl_3) δ 10.50.

HRMS (ESI $^-$) m/z theoretical for $\text{C}_{32}\text{H}_{16}\text{ClF}_{52}\text{Sn} = 1542.9136$, found $[\text{M}+\text{Cl}]^- = 1542.9104$.

Synthesis of $(\text{C}_6\text{F}_{13}\text{C}_2\text{H}_4)_3\text{SnCl}$ (**2b**). As stated in the literature,² phenyltin trichloride (1.87 g, 6.22 mmol) solution in dry toluene (12 mL) was added dropwise to the Grignard reagent $\text{C}_6\text{F}_{13}\text{C}_2\text{H}_4\text{MgI}$, prepared as previously mentioned. The reaction was refluxed for 4 h and stirred overnight at ambient temperature. The reaction was hydrolyzed by the slow addition of NH_4Cl solution and then filtrated through a Celite pad. The organic phase was washed with 5% $\text{Na}_2\text{S}_2\text{O}_3$ solution and deionized water, dried over MgSO_4 , and concentrated by rotary evaporation. The crude product was finally purified by the classical column chromatography on silica gel using hexane to give $(\text{C}_6\text{F}_{13}\text{C}_2\text{H}_4)_3\text{SnPh}$ (48.7% yield) as a colorless oil.

^1H NMR (300.2 MHz, CDCl_3) δ 1.30 (t, 6H, $^3J_{\text{H-H}} = 8$ Hz, $^2J_{\text{Sn-H}} = 55$ Hz), 2.31 (tt, 6H, $^3J_{\text{F-H}} = 18$ Hz, $^3J_{\text{H-H}} = 8$ Hz), 7.39 (m, 5 H); ^{19}F NMR (282.4 MHz, CDCl_3) δ - 80.90 (t, 9F), -116.56 (m, 6F), -122.00 (m, 6F), -122.96 (m, 6F), -123.51 (m, 6F), -126.25 (m, 6F); ^{13}C NMR (75 MHz, CDCl_3) δ -1.56 (s, $^1J_{\text{C-Sn}} = 170$ Hz), 27.65 (t, $^2J_{\text{C-F}} = 23$ Hz), 136.40 (1C, quaternary), 135.95 (2C, $^2J_{\text{Sn-C}} = 17$ Hz), 129.53 (1C, $^4J_{\text{Sn-C}} = 6$ Hz) 128.95 (2C, $^3J_{\text{Sn-C}} = 25$ Hz); ^{119}Sn NMR (223.8 MHz, CDCl_3) δ -28.64.

TMSCl (7.5 mmol, 0.95 mL) was added at 0 °C to a CCl₄ solution (15 mL) containing (C₆F₁₃C₂H₄)₃SnPh (5 mmol, 6.18 g) and dry MeOH (25 mmol, 1 mL). The reaction mixture was stirred overnight at ambient temperature.¹ The solution was evaporated, and the crude product was subjected to column chromatography on silica gel using dichloromethane as an eluent to give **2b** as a colorless oil (5.49 g, 40%).

¹H NMR (300.2 MHz, CDCl₃) δ 1.52 (t, 6H, ³J_{H-H} = 8 Hz, ²J_{Sn-H} = 55 Hz), 2.46 (tt, 6H, ³J_{F-H} = 18 Hz, ³J_{H-H} = 8 Hz); ¹⁹F NMR (282.4 MHz, CDCl₃) δ -80.89 (t, 9F), -116.02 (m, 6F), -121.95 (m, 6F), -122.93 (m, 6F), -123.49 (m, 6F), -126.22 (m, 6F); ¹³C NMR (75 MHz, CDCl₃) δ 6.26 (s, ¹J_{C-Sn} = 190 Hz), 26.85 (t, ²J_{C-F} = 23 Hz); ¹¹⁹Sn NMR (223.8 MHz, CDCl₃) δ 123.98.

HRMS (MALDI-TOF) m/z theoretical for C₂₄H₁₂ClF₃₉NaSn = 1218.892, found [M+Na]⁺ = 1218.956.

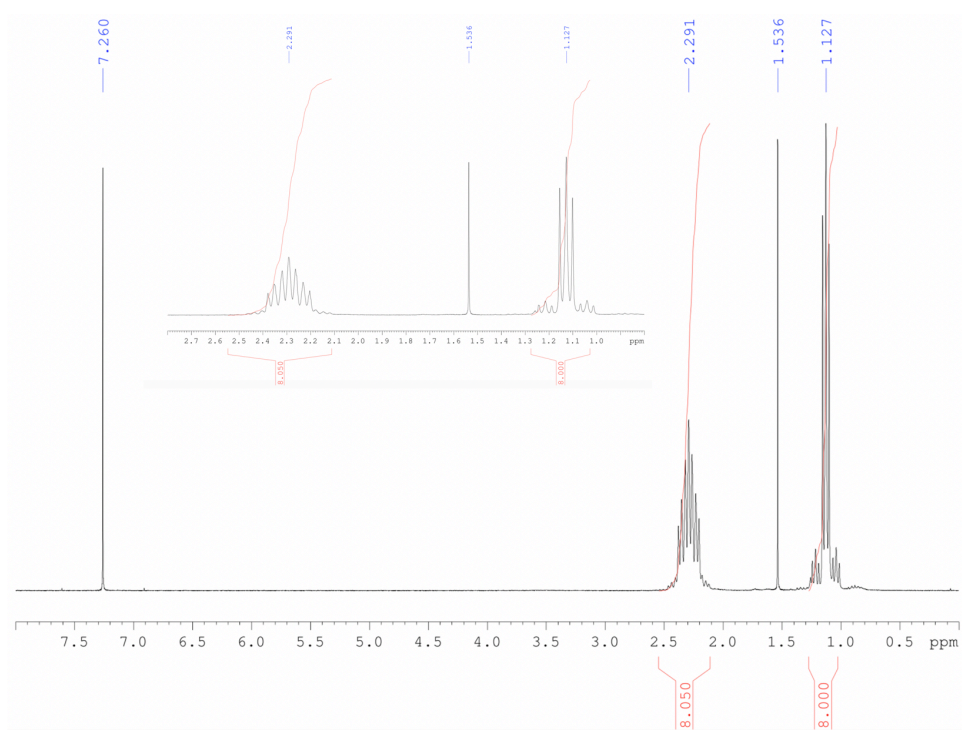


Figure S1. ¹H NMR spectrum of **1a** (300.2 MHz, CDCl₃).

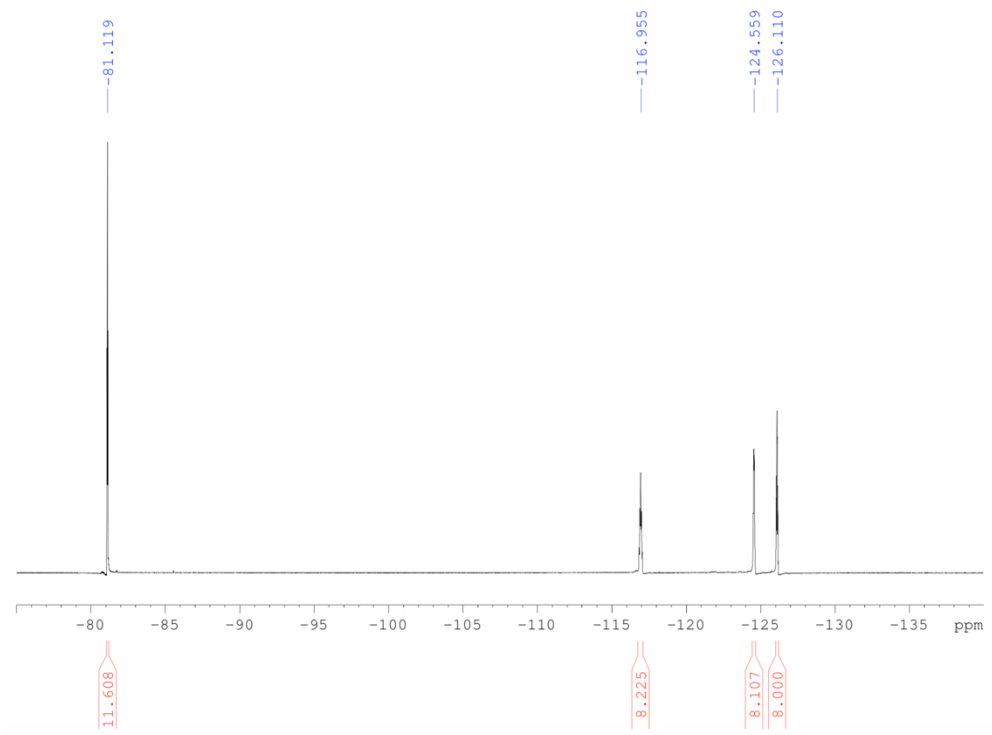


Figure S2. ^{19}F NMR spectrum of **1a** (282.4 MHz, CDCl_3).

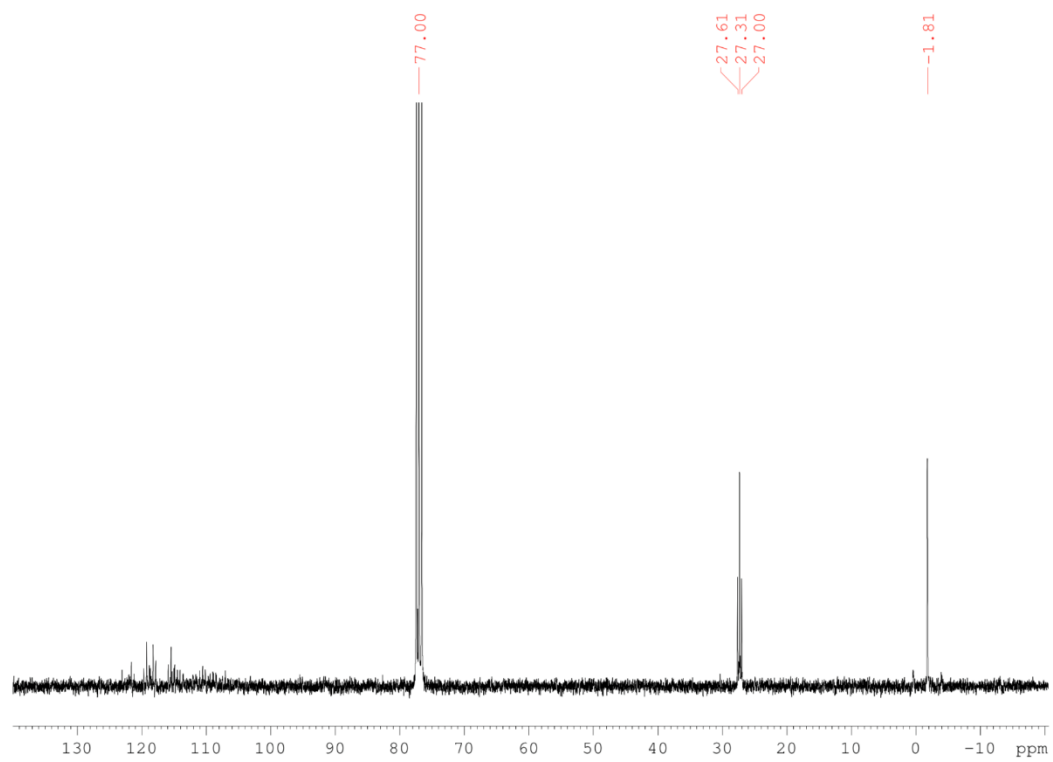


Figure S3. ^{13}C NMR spectrum of **1a** (75 MHz, CDCl_3).

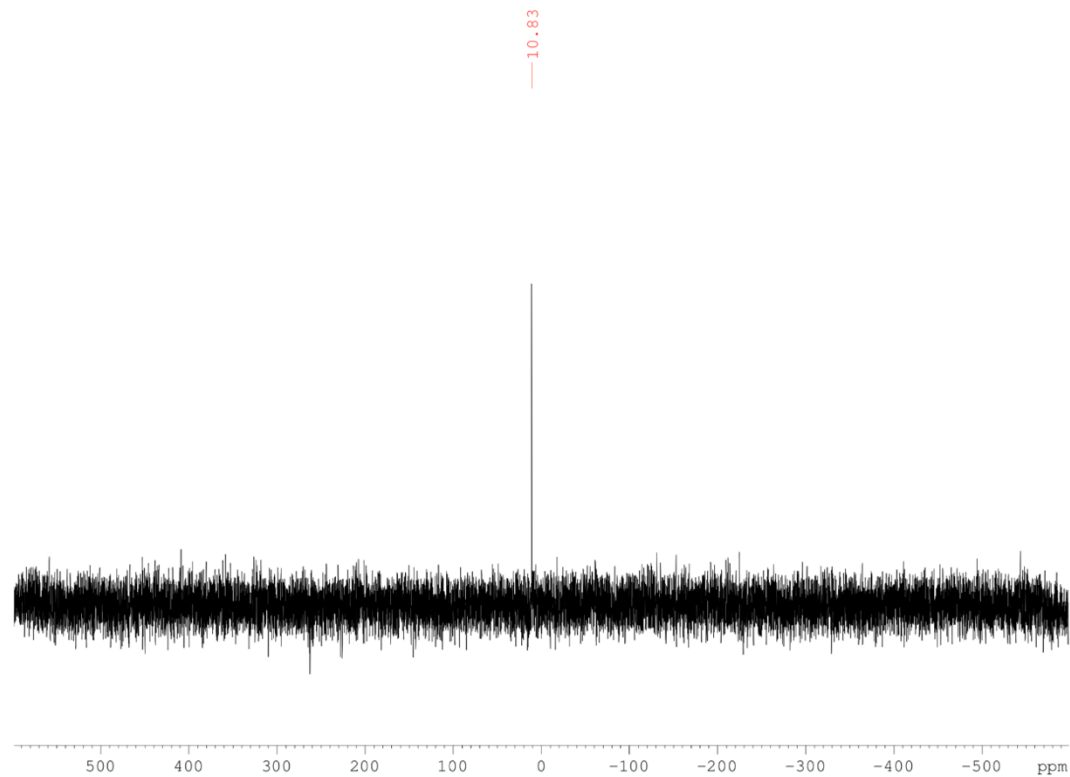


Figure S4. ^{119}Sn NMR spectrum of **1a** (223.8 MHz, CDCl_3).

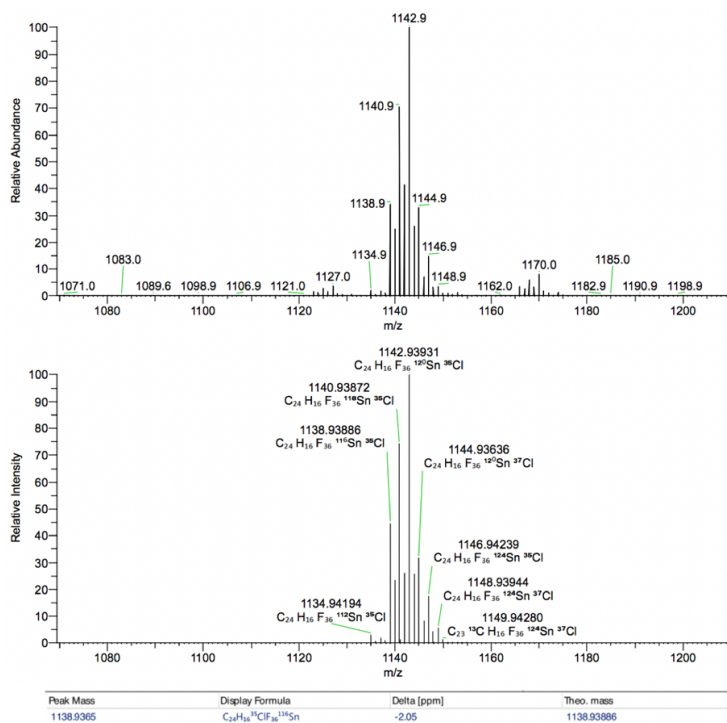


Figure S5. ESI spectrum of **1a** in CHCl_3 .

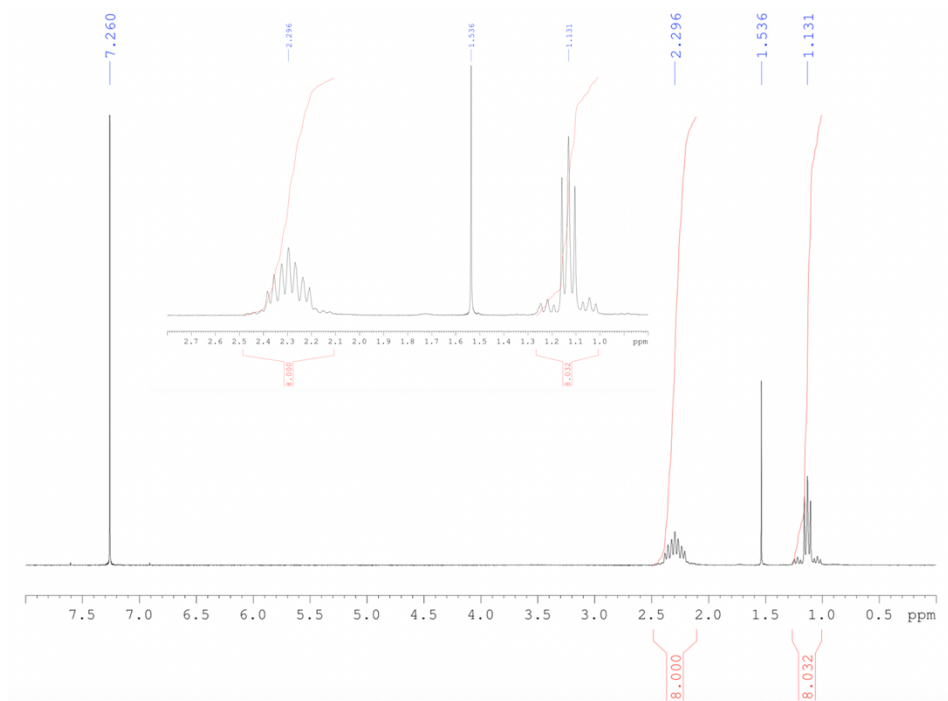


Figure S6. ^1H NMR spectrum of **1b** (300.2 MHz, CDCl_3).

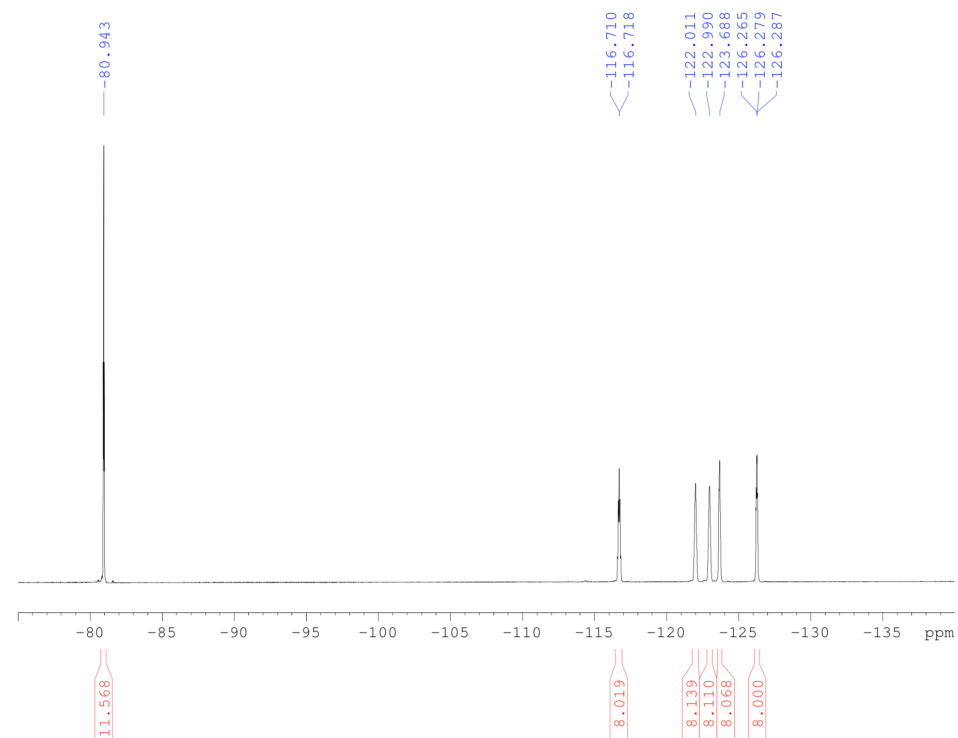


Figure S7. ^{19}F NMR spectrum of **1b** (282.4 MHz, CDCl_3).

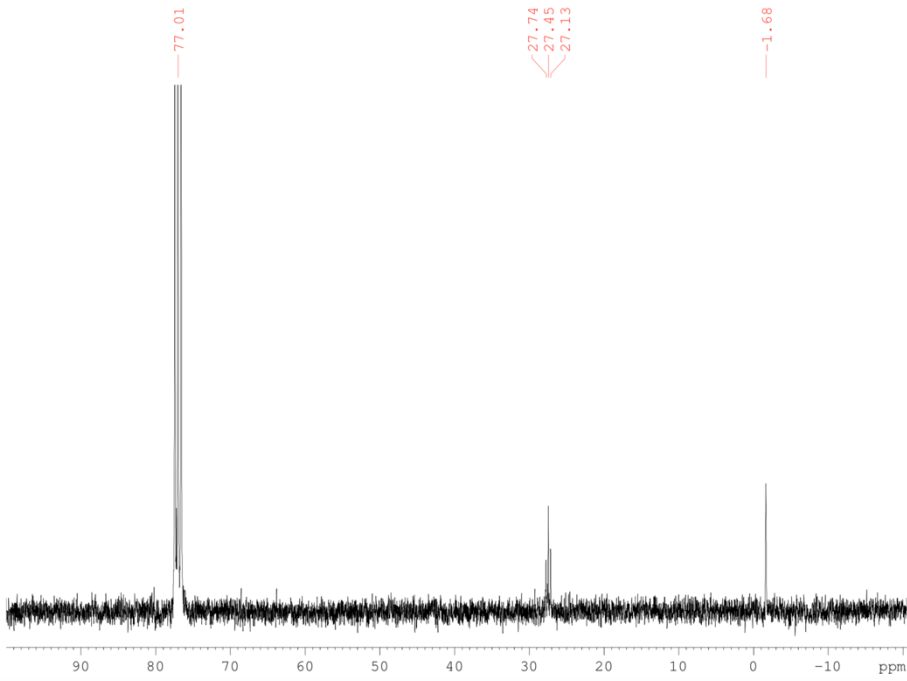


Figure S8. ^{13}C NMR spectrum of **1b** (75 MHz, CDCl_3).

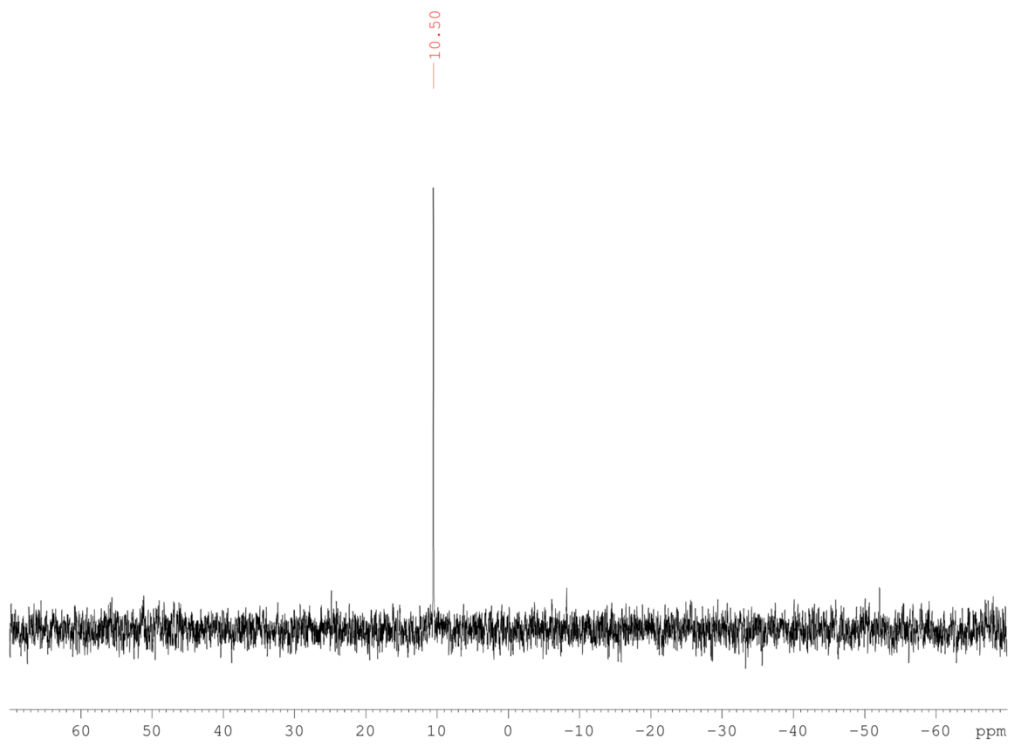


Figure S9. ^{119}Sn NMR spectrum of **1b** (223.8 MHz, CDCl_3).

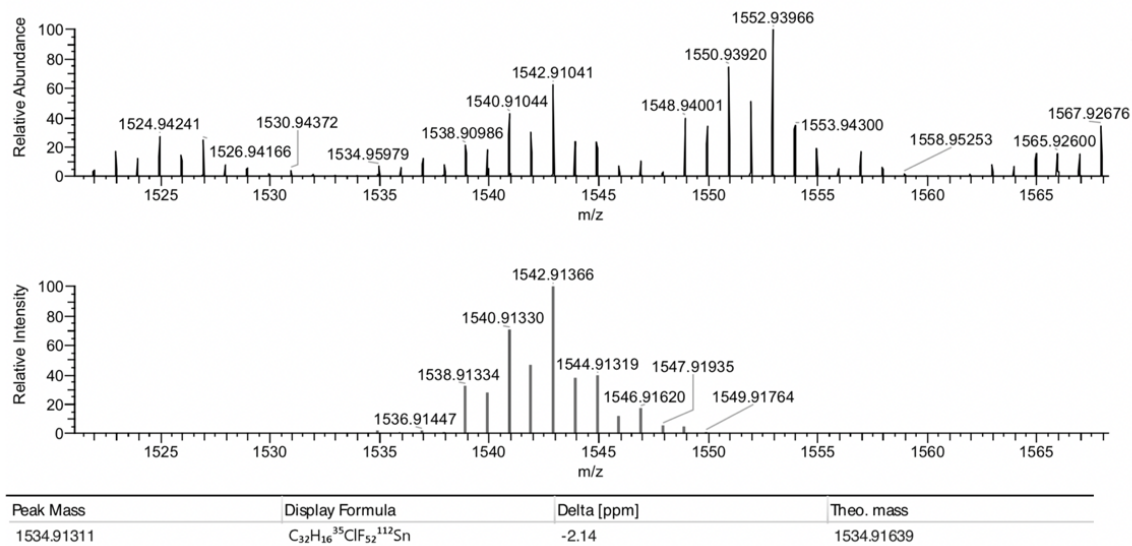


Figure S10. ESI spectrum of **1b** in CHCl₃.

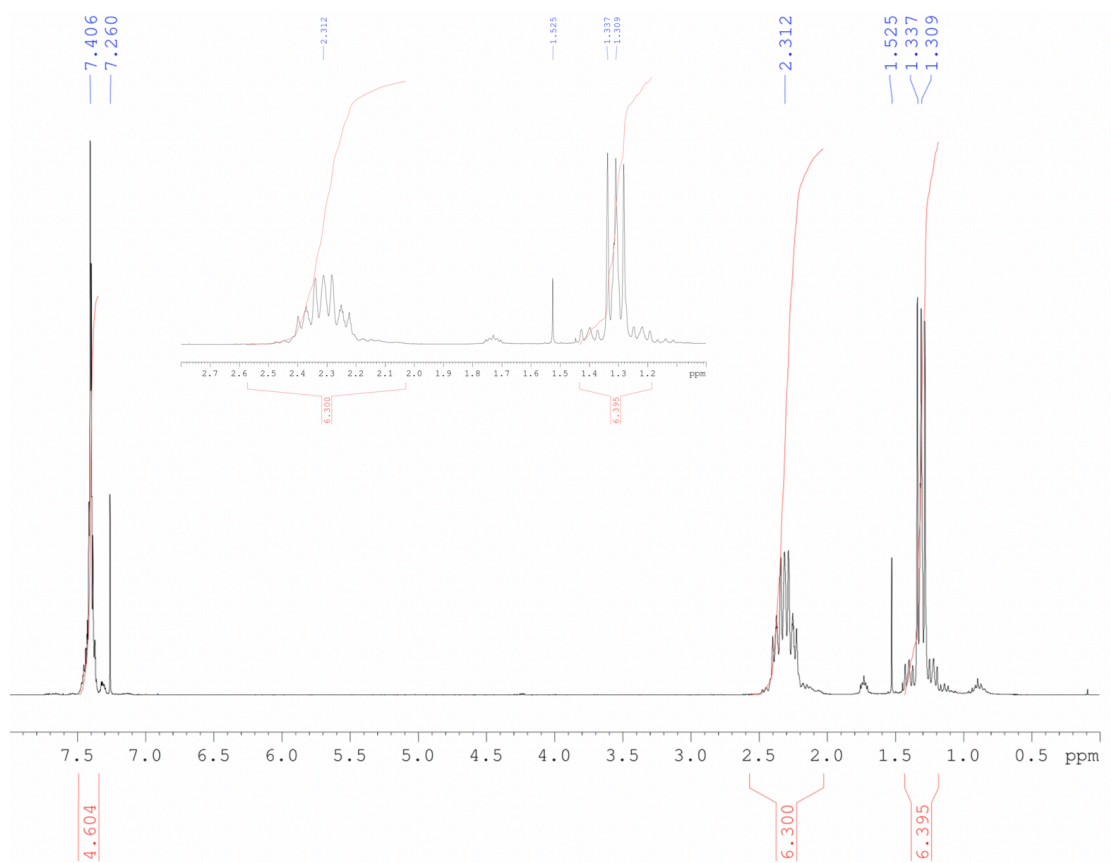


Figure S11. ¹H NMR spectrum of (C₄F₉C₂H₄)₃SnPh (300.2 MHz, CDCl₃).

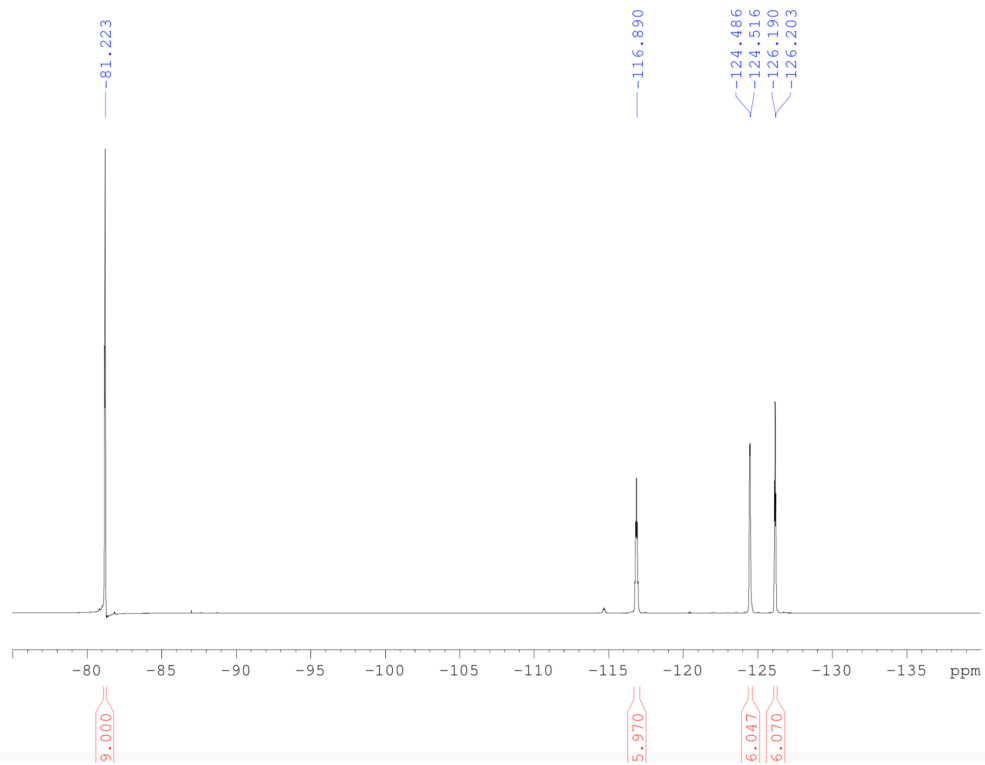


Figure S12. ^{19}F NMR spectrum of $(\text{C}_4\text{F}_9\text{C}_2\text{H}_4)_3\text{SnPh}$ (282.4 MHz, CDCl_3).

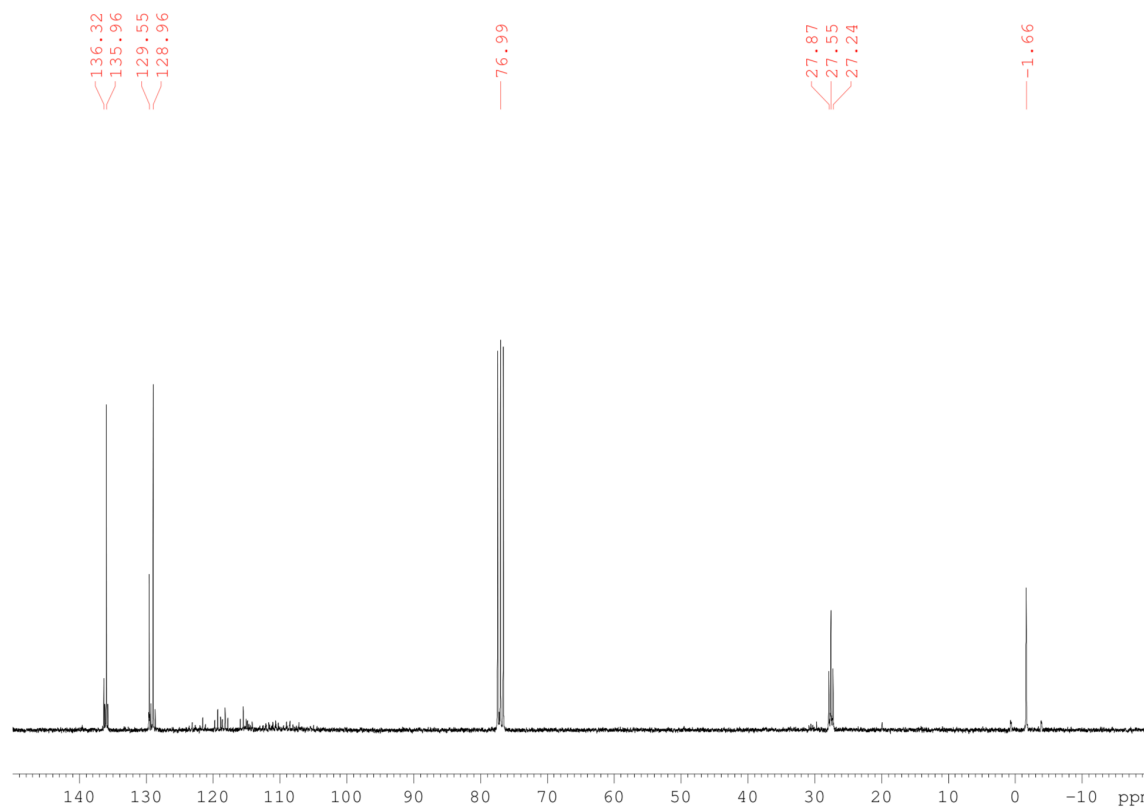


Figure S13. ^{13}C NMR spectrum of $(\text{C}_4\text{F}_9\text{C}_2\text{H}_4)_3\text{SnPh}$ (75 MHz, CDCl_3).

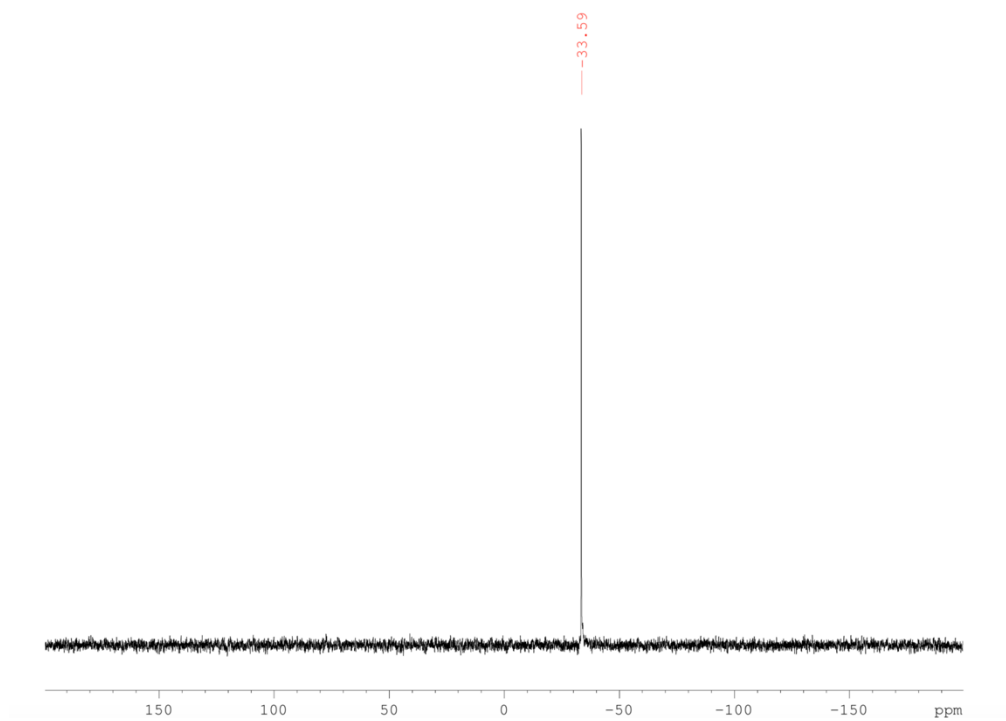


Figure S14. ^{119}Sn NMR spectrum of $(\text{C}_4\text{F}_9\text{C}_2\text{H}_4)_3\text{SnPh}$ (223.8 MHz, CDCl_3).

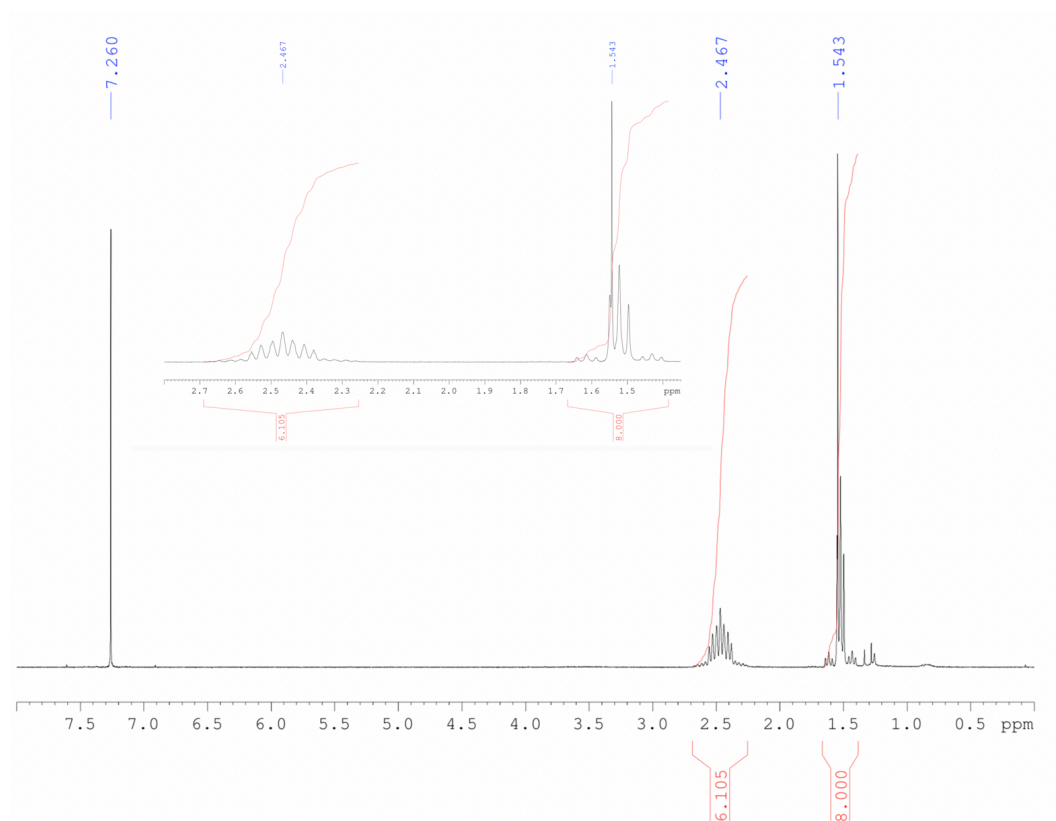


Figure S15. ^1H NMR spectrum of **2a** (300.2 MHz, CDCl_3).

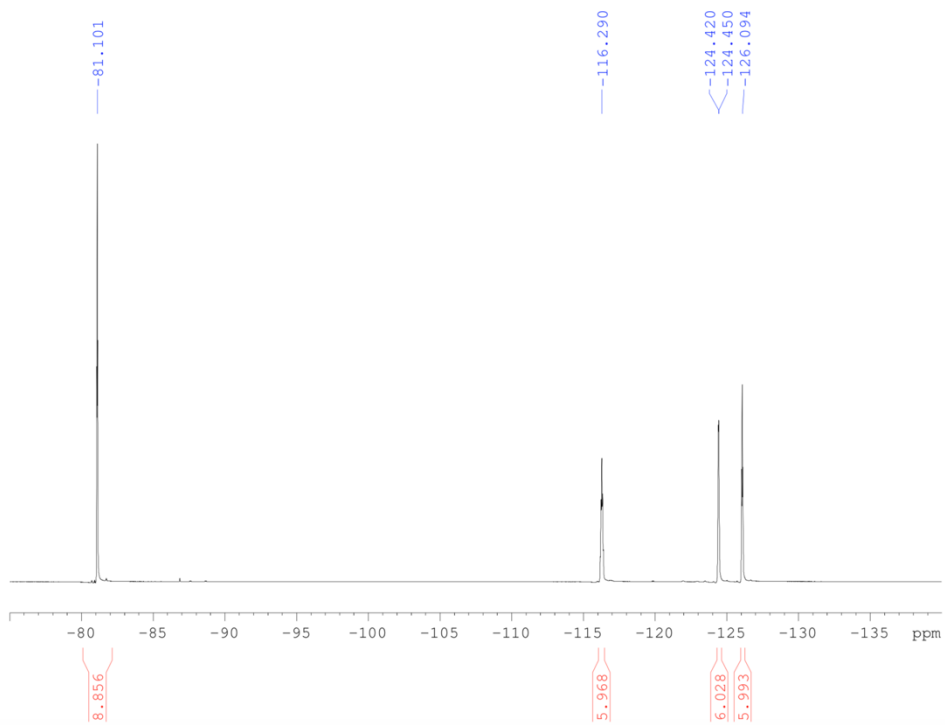


Figure S16. ^{19}F NMR spectrum of **2a** (282.4 MHz, CDCl_3).

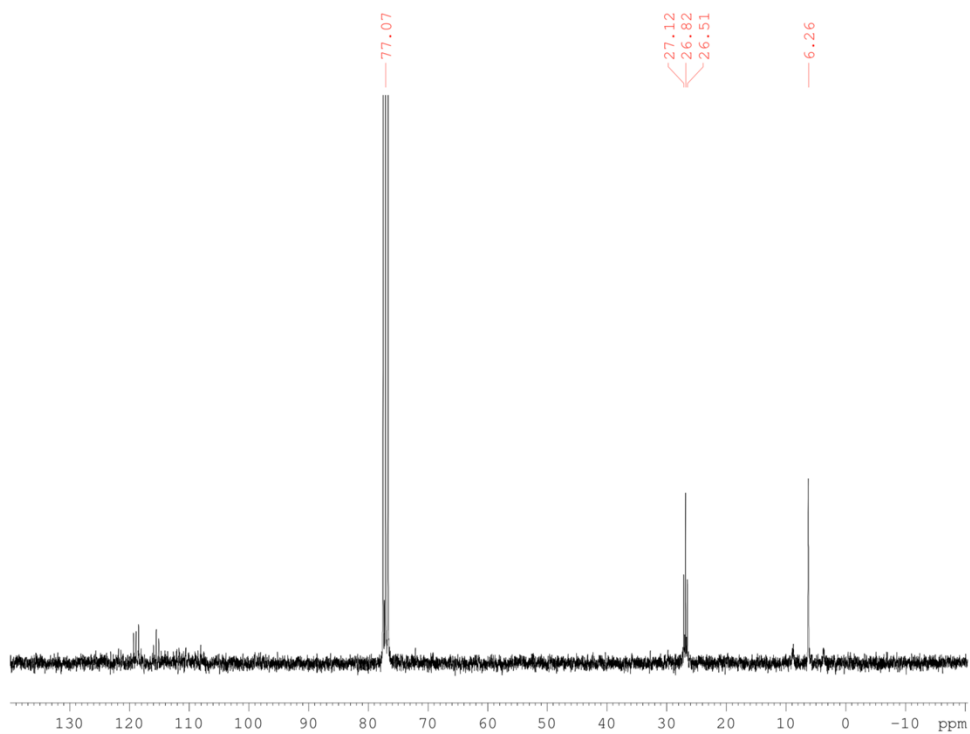


Figure S17. ^{13}C NMR spectrum of **2a** (75 MHz, CDCl_3).

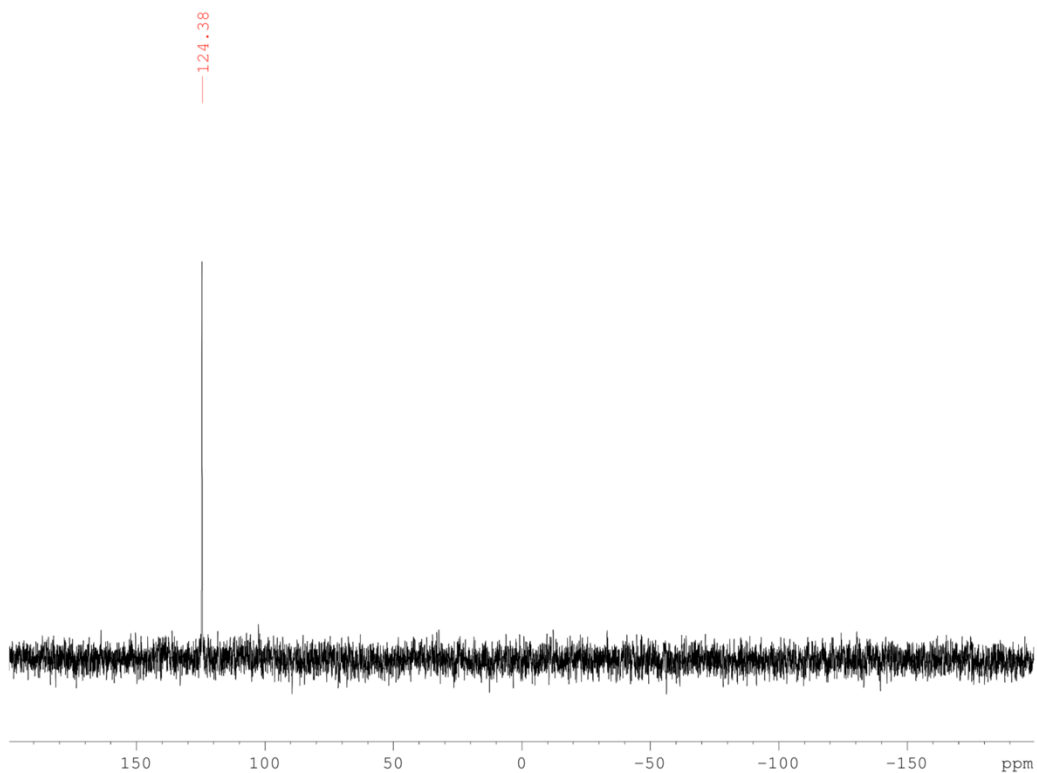


Figure S18. ^{119}Sn NMR spectrum of **2a** (223.8 MHz, CDCl_3).

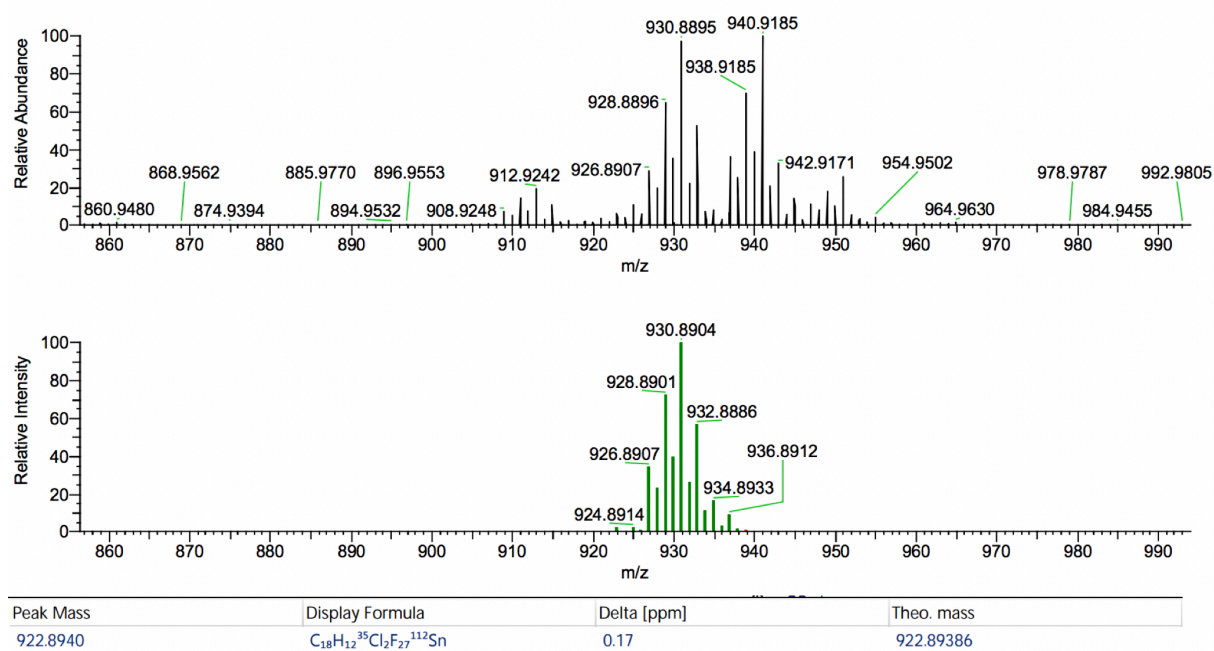


Figure S19. ESI spectrum of **2a** in CHCl_3 .

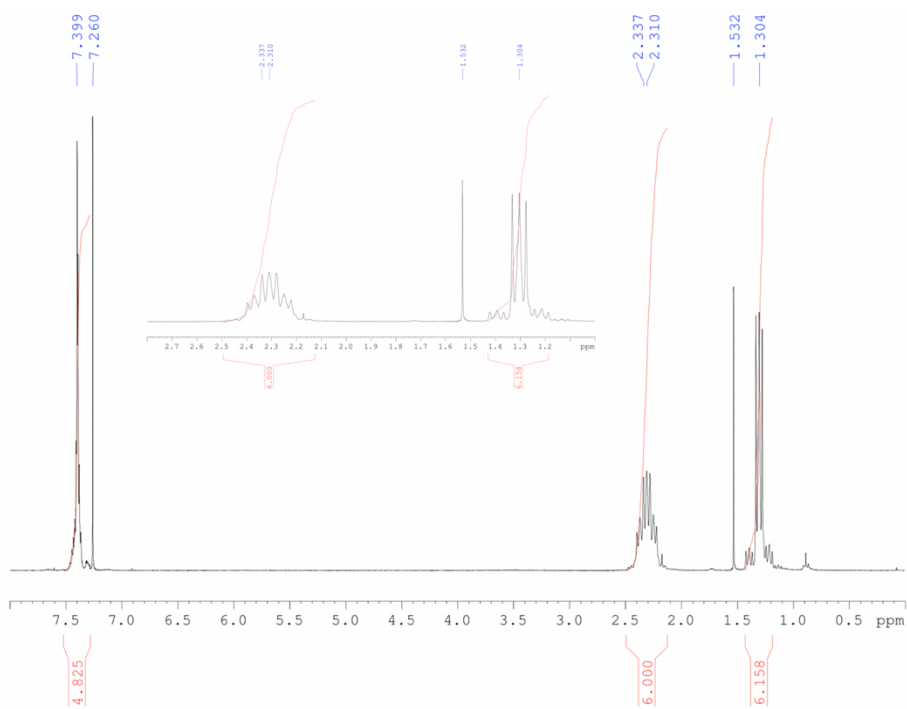


Figure S20. ^1H NMR spectrum of $(\text{C}_6\text{F}_{13}\text{C}_2\text{H}_4)_3\text{SnPh}$ (300.2 MHz, CDCl_3).

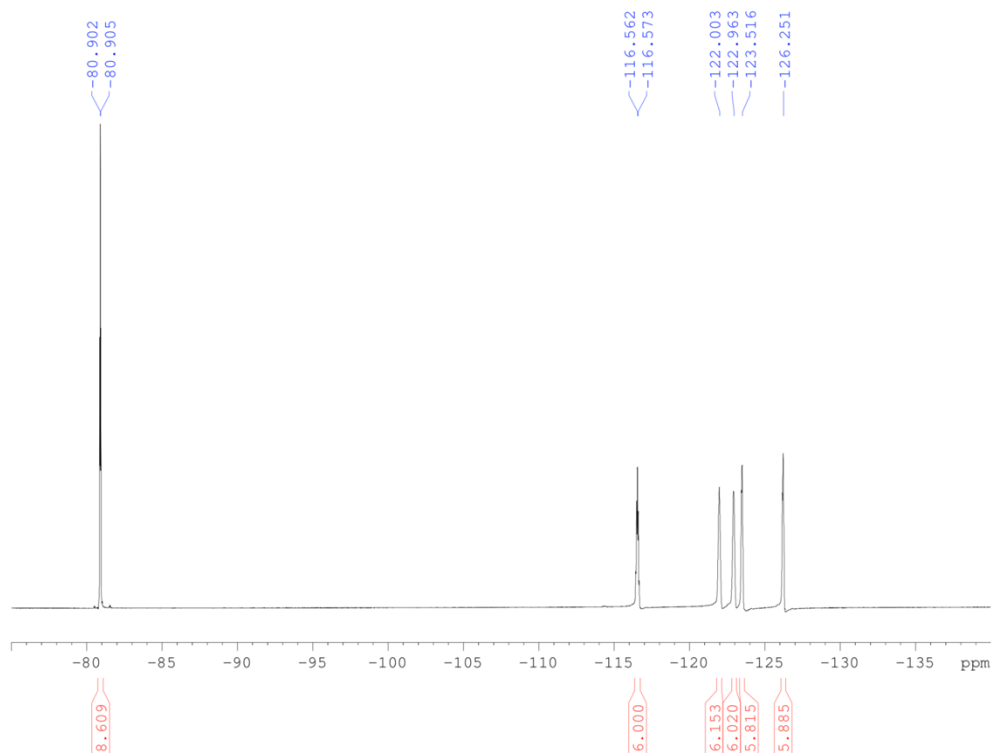


Figure S21. ^{19}F NMR spectrum of $(\text{C}_6\text{F}_{13}\text{C}_2\text{H}_4)_3\text{SnPh}$ (282.4 MHz, CDCl_3).

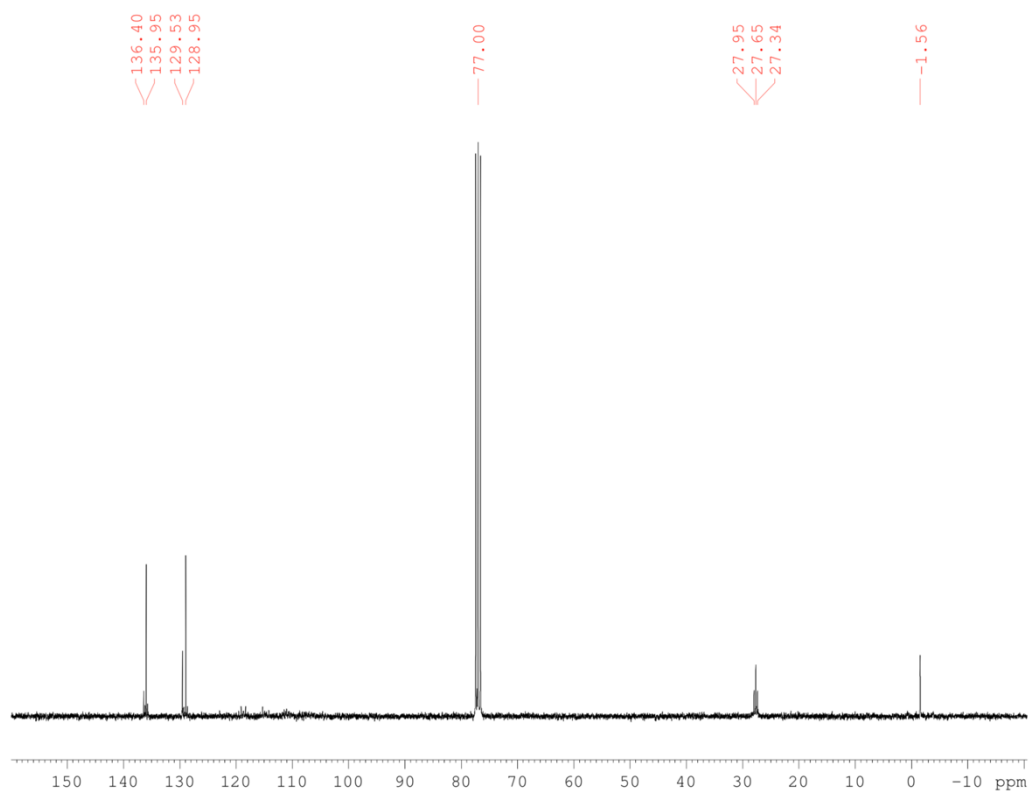


Figure S22. ^{13}C NMR spectrum of $(\text{C}_6\text{F}_{13}\text{C}_2\text{H}_4)_3\text{SnPh}$ (75 MHz, CDCl_3).

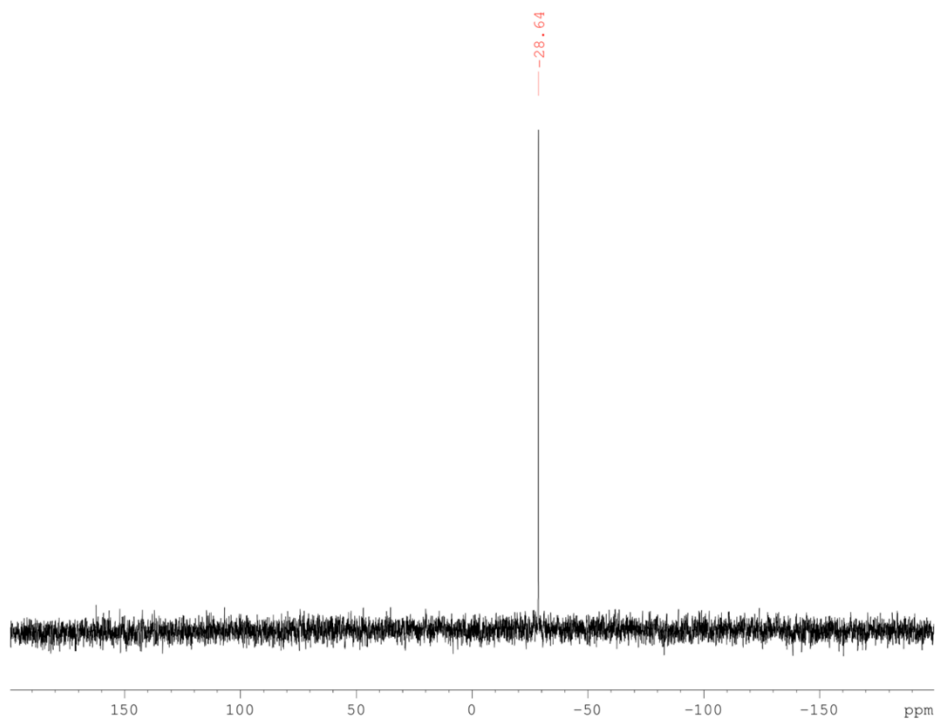


Figure S23. ^{119}Sn NMR spectrum of $(\text{C}_6\text{F}_{13}\text{C}_2\text{H}_4)_3\text{SnPh}$ (223.8 MHz, CDCl_3).

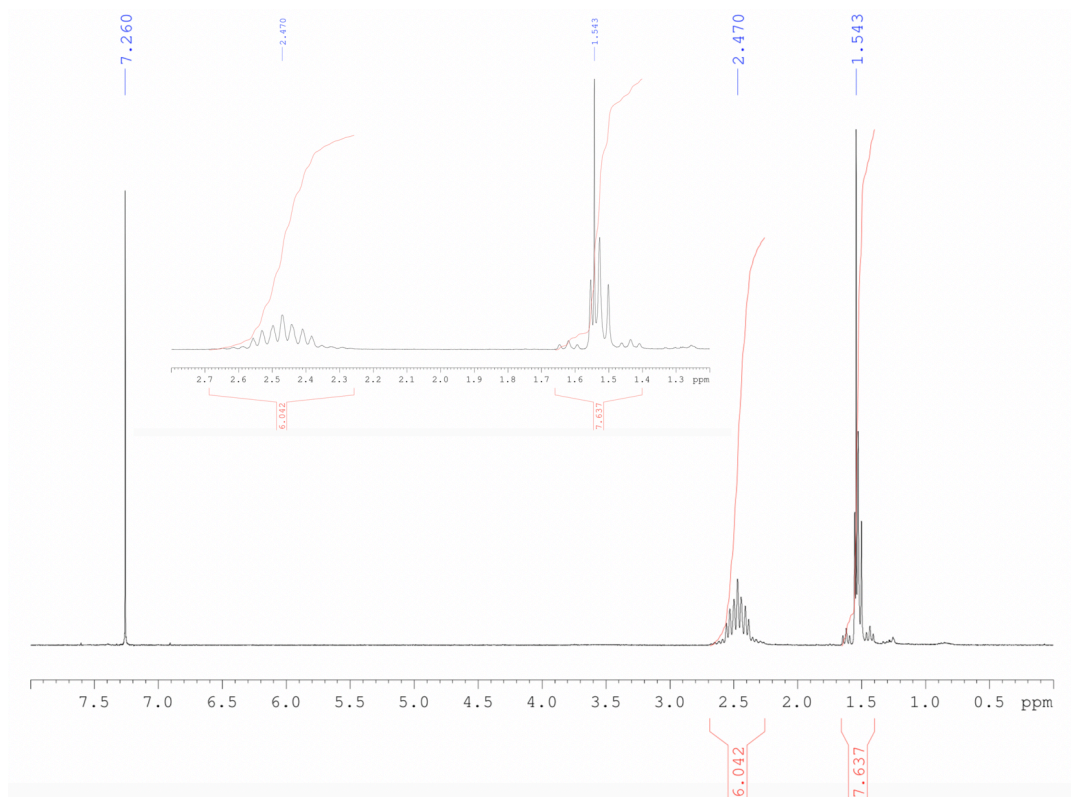


Figure S24. ^1H NMR spectrum of **2b** (300.2 MHz, CDCl_3).

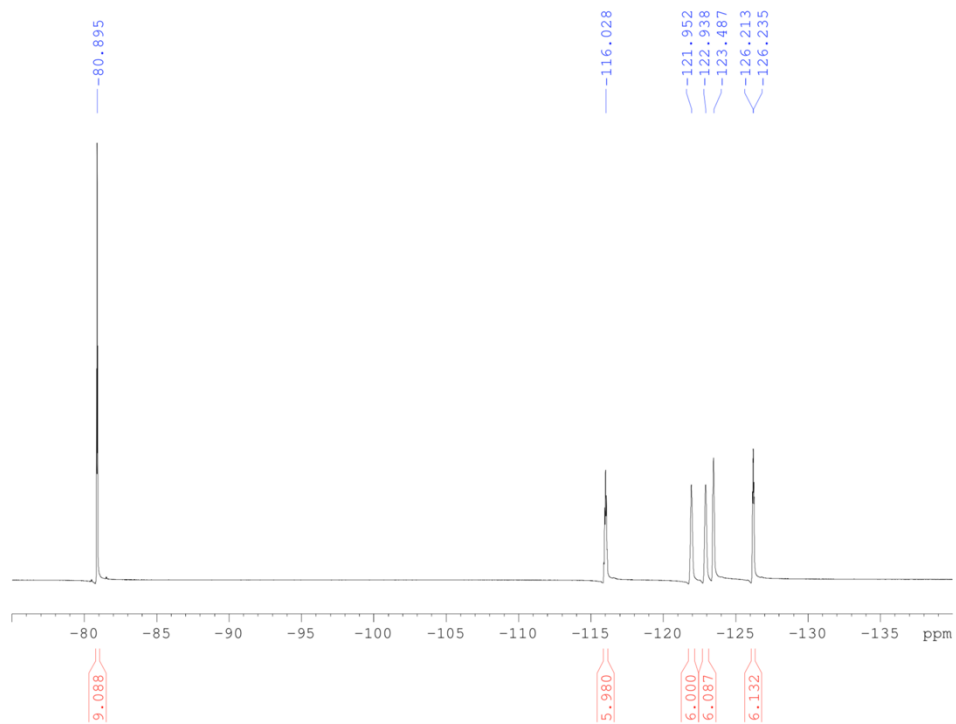


Figure S25. ^{19}F NMR spectrum of **2b** (282.4 MHz, CDCl_3).

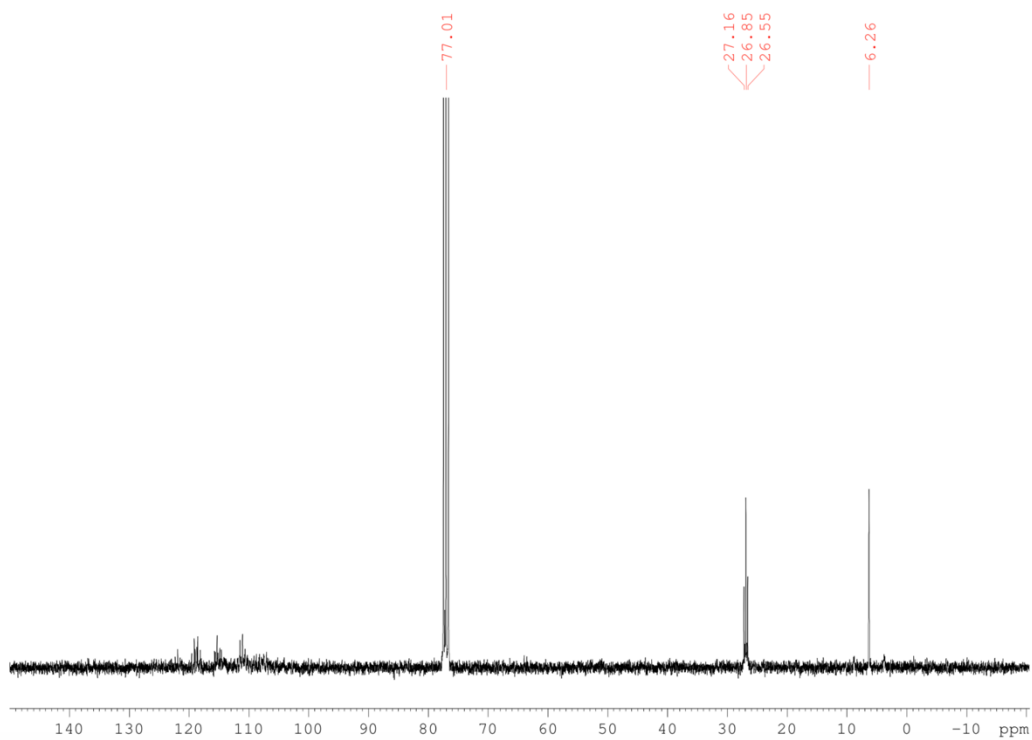


Figure S26. ^{13}C NMR spectrum of **2b** (75 MHz, CDCl_3).

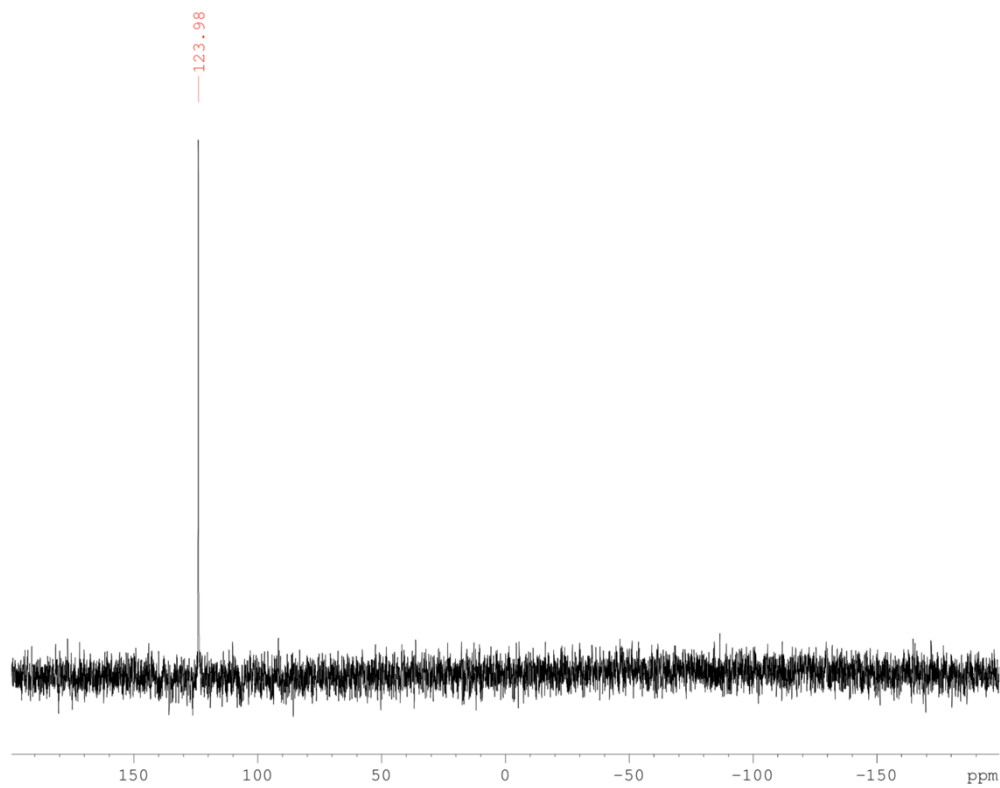


Figure S27. ^{119}Sn NMR spectrum of **2b** (223.8 MHz, CDCl_3).

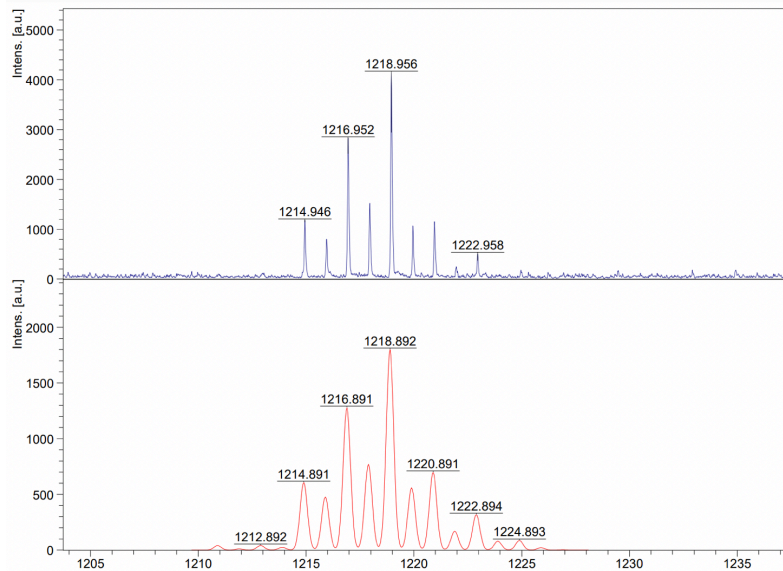


Figure S28. MALDI-TOF spectrum of **2b** in CHCl_3 .

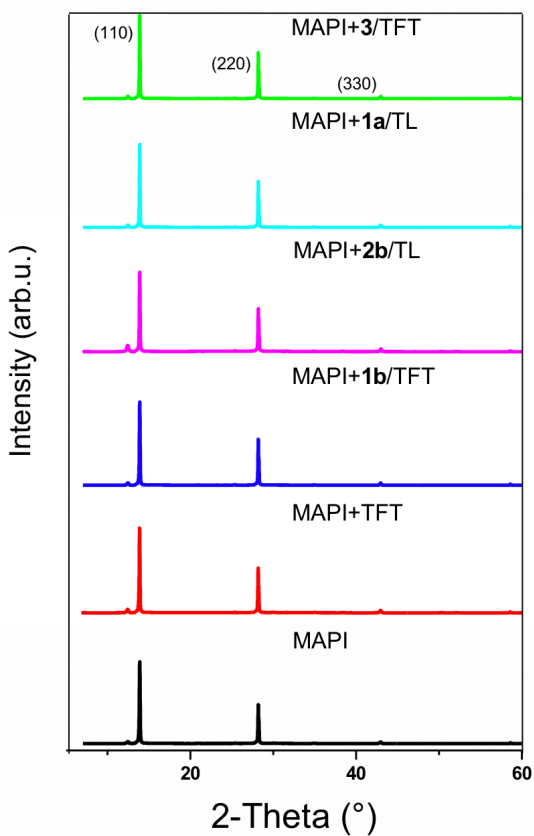


Figure S29. Characteristic tetragonal phase XRD pattern of pristine and modified MAPI samples.

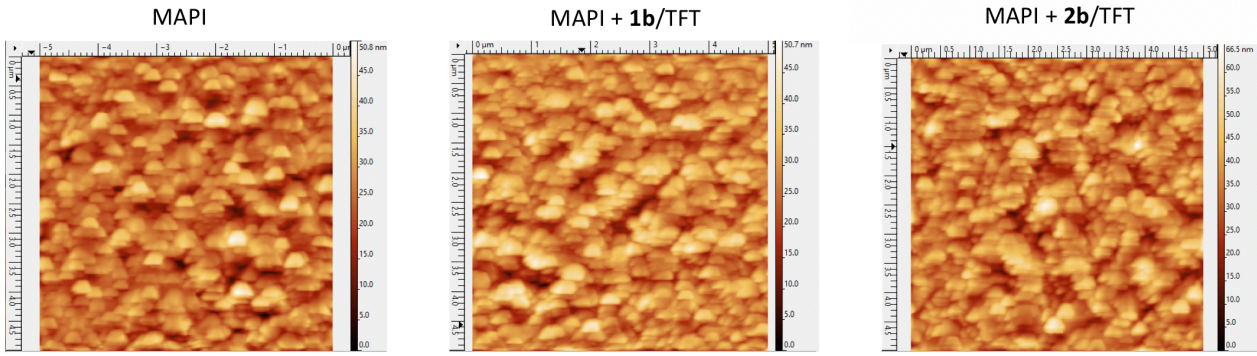


Figure S30. AFM images of pristine and modified MAPI surfaces.

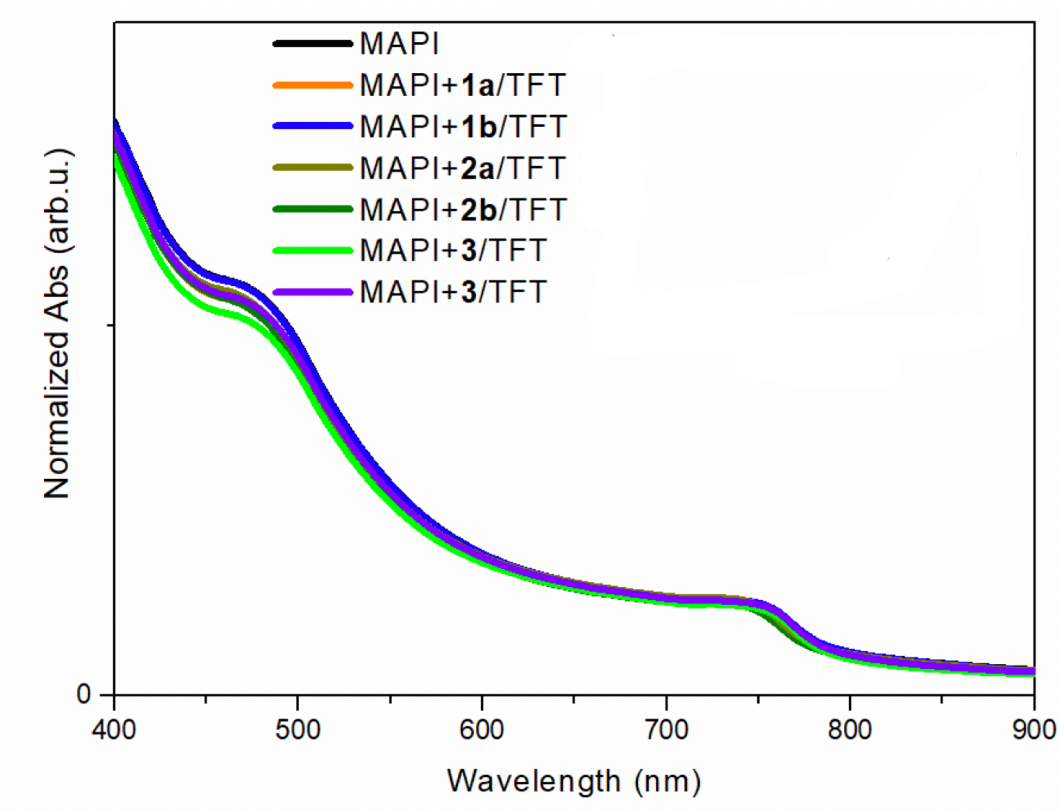


Figure S31. Normalized Abs spectra of pristine and modified MAPI surfaces.

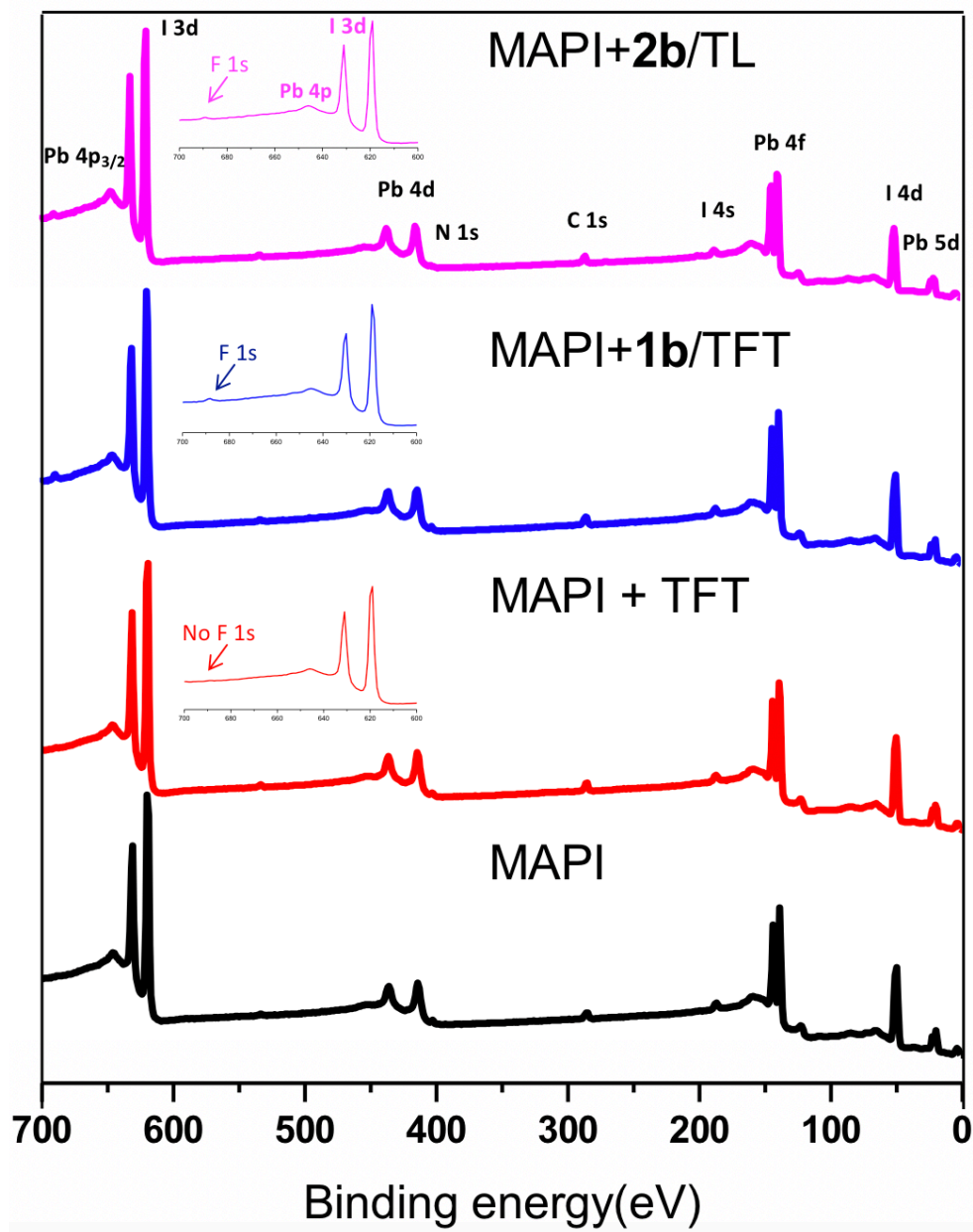
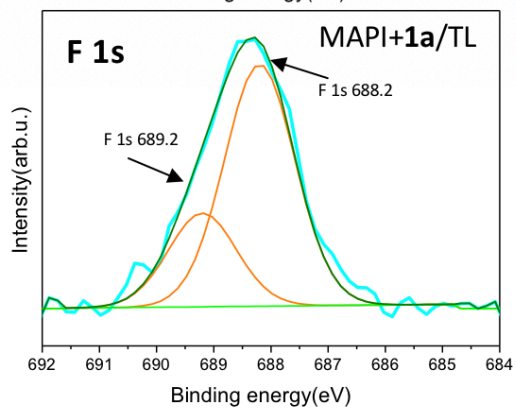
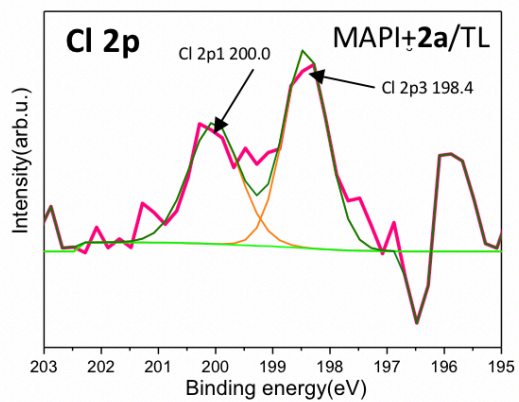
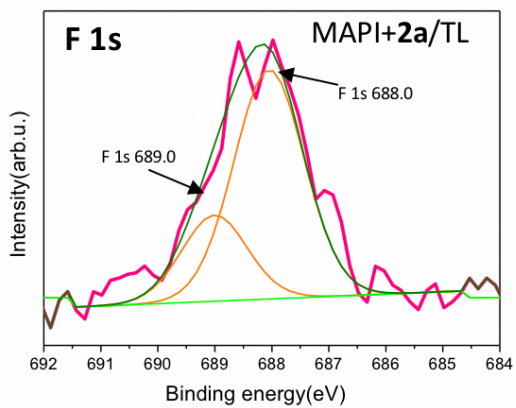
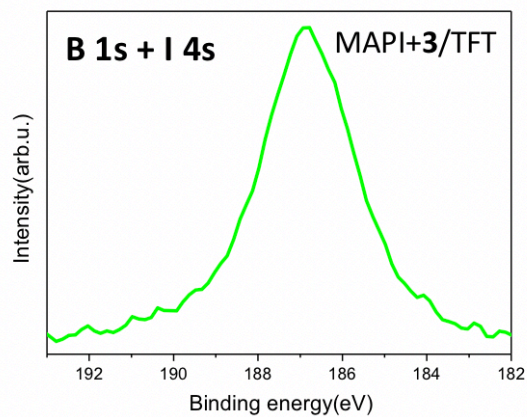
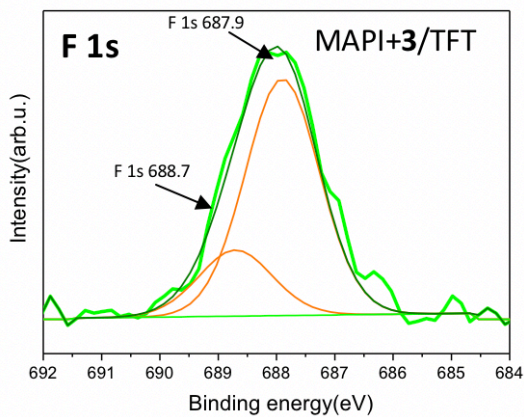
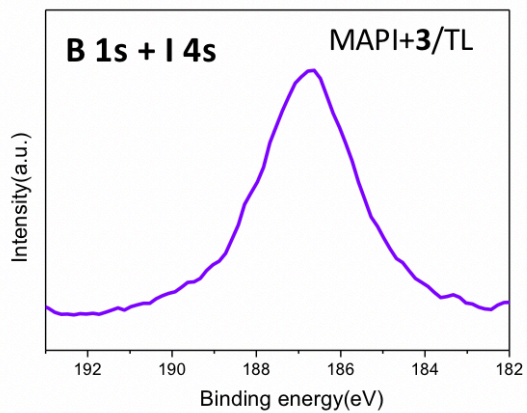
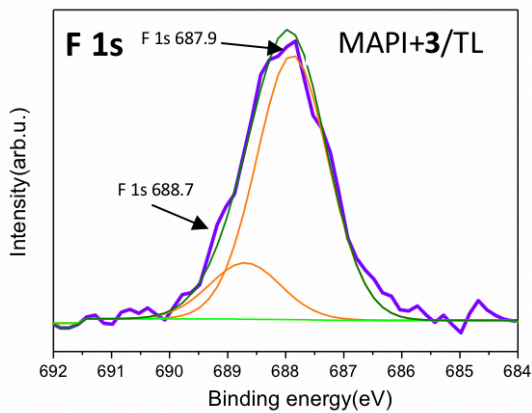


Figure S32. Overview XPS spectra measured for pristine and modified MAPI surfaces.



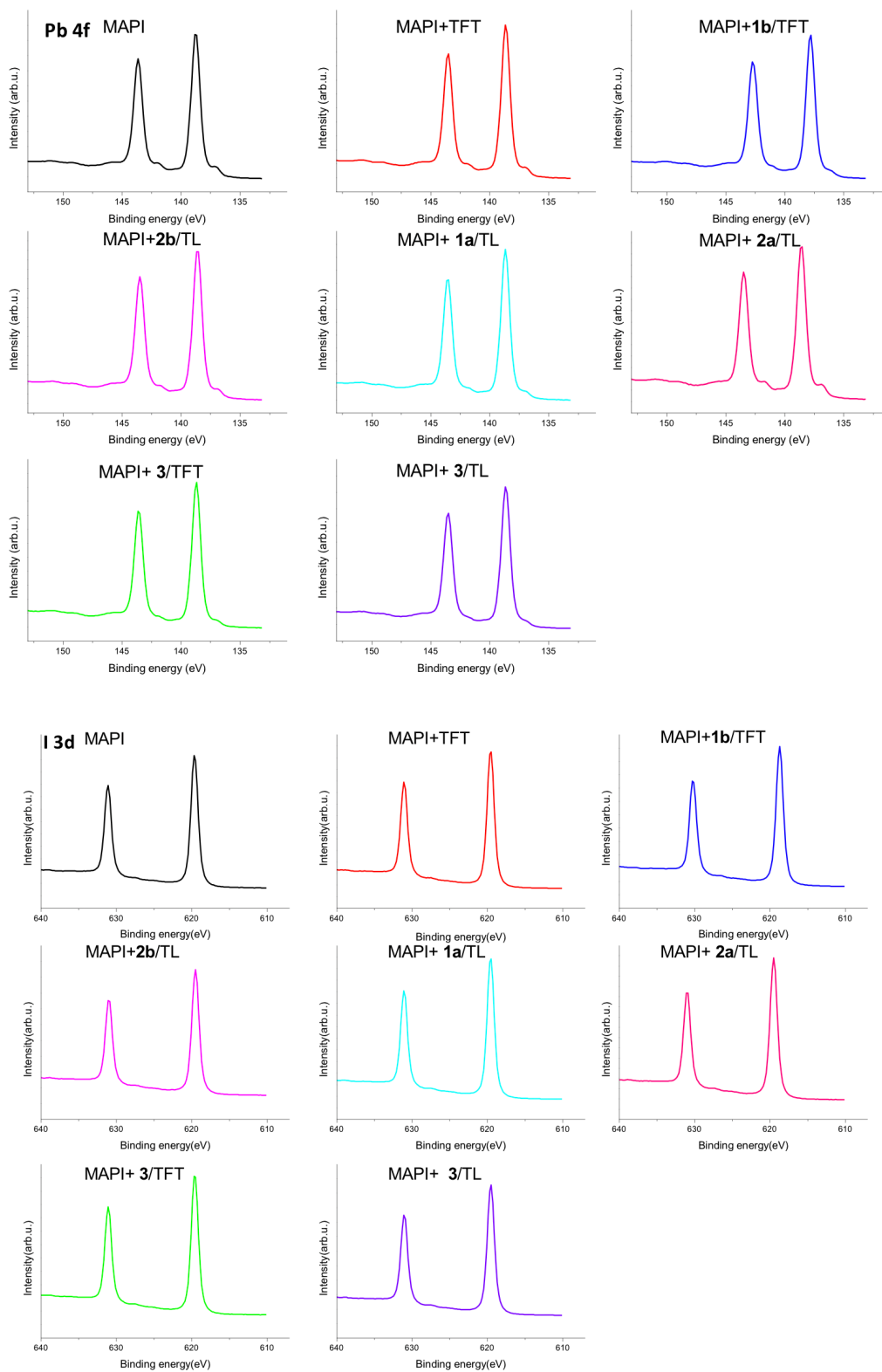


Figure S33. XPS spectra of fitted F 1s, B 1s-I 4s, fitted Cl 2p, Pb 4f and I 3d for pristine and different passivated perovskite surfaces.

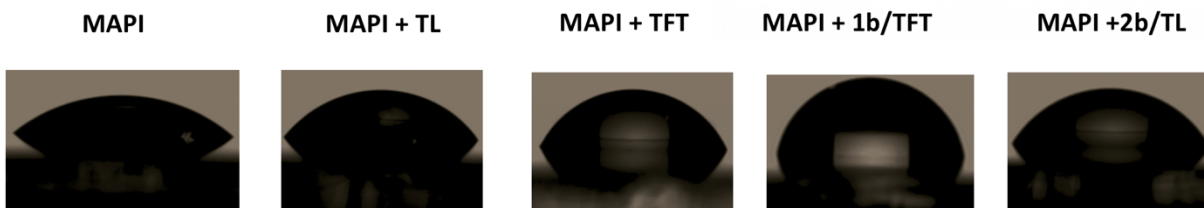


Figure S34. Contact angle measurements of water on pristine and modified perovskite surfaces.

Table S1. Calculated molecular dipole moments (μ) of **1** – **3**.^a

Compound	1a	1b	2a	2b	3
μ (Debye)	0.384	0.301	0.824	0.780	< 0.001

^aCalculated using a PM3 semi-empirical Hamiltonian at the MM+ geometry.

ATR experiments, determination of the optical constants and spectral simulation of the IRRAS spectrum for a compact monolayer

The polarized ATR spectra of **1a**, **1b**, **2a**, **2b** and **3** compounds were recorded on a ThermoScientific iS50 FTIR spectrometer at a resolution of 4 cm^{-1} , by coadding 500 scans. ATR experiments were performed using a single-reflection ATR accessory (Specac) equipped with a germanium (Ge) crystal and a DTGS detector. A BaF_2 wire grid polarizer was added to record the spectra in the *p*- and *s*-polarizations. **1a**, **1b**, **2a**, **2b** and **3** films were obtained after successive evaporation of $10\ \mu\text{l}$ of chloroform-based solutions. The isotropic and anisotropic optical constants (refractive index $n(\bar{\nu})$ and extinction coefficient $k(\bar{\nu})$) of **1a**, **1b**, **2a**, **2b** and **3** compounds have been determined from polarized ATR spectra, using the procedure described by Dignam et al.³ Isotropic optical constants (i.e. similar values of the in-plane and out-of-plane refractive indexes and extinction coefficients) have been measured for **1a**, **1b**, **2a**, **2b** and **3** compounds. We have checked for these three compounds that the intensities of the bands in the *p*-polarized ATR spectrum are the double than those measured in the *s*-polarized ATR spectrum, that is expected for

an isotropic layer. The refractive index in the visible was set to 1.33 for **1a**, **1b**, **2a**, **2b** and to 1.41 for **3**. The computer program used to calculate the IRRAS spectra for a compact monolayer of **1a**, **1b**, **2a**, **2b** and **3** compounds deposited onto perovskite/Au substrate is based on the Abeles' matrix formalism,^{4,5} which has been generalized for anisotropic layers.⁶ Several parameters must be fixed in the program such as the thickness of the monolayer, the refractive index (set to 2.5) and the thickness (set to 185 nm) of the perovskite film, the angle of incidence (set to 75°) and the polarization of the infrared beam. The *p*-polarized reflectance of the covered $R_p(d)$ and bare $R_p(0)$ substrates have been calculated using the spectral dependence of the optical constants of **1a**, **1b**, **2a**, **2b** and **3** and of gold.⁷

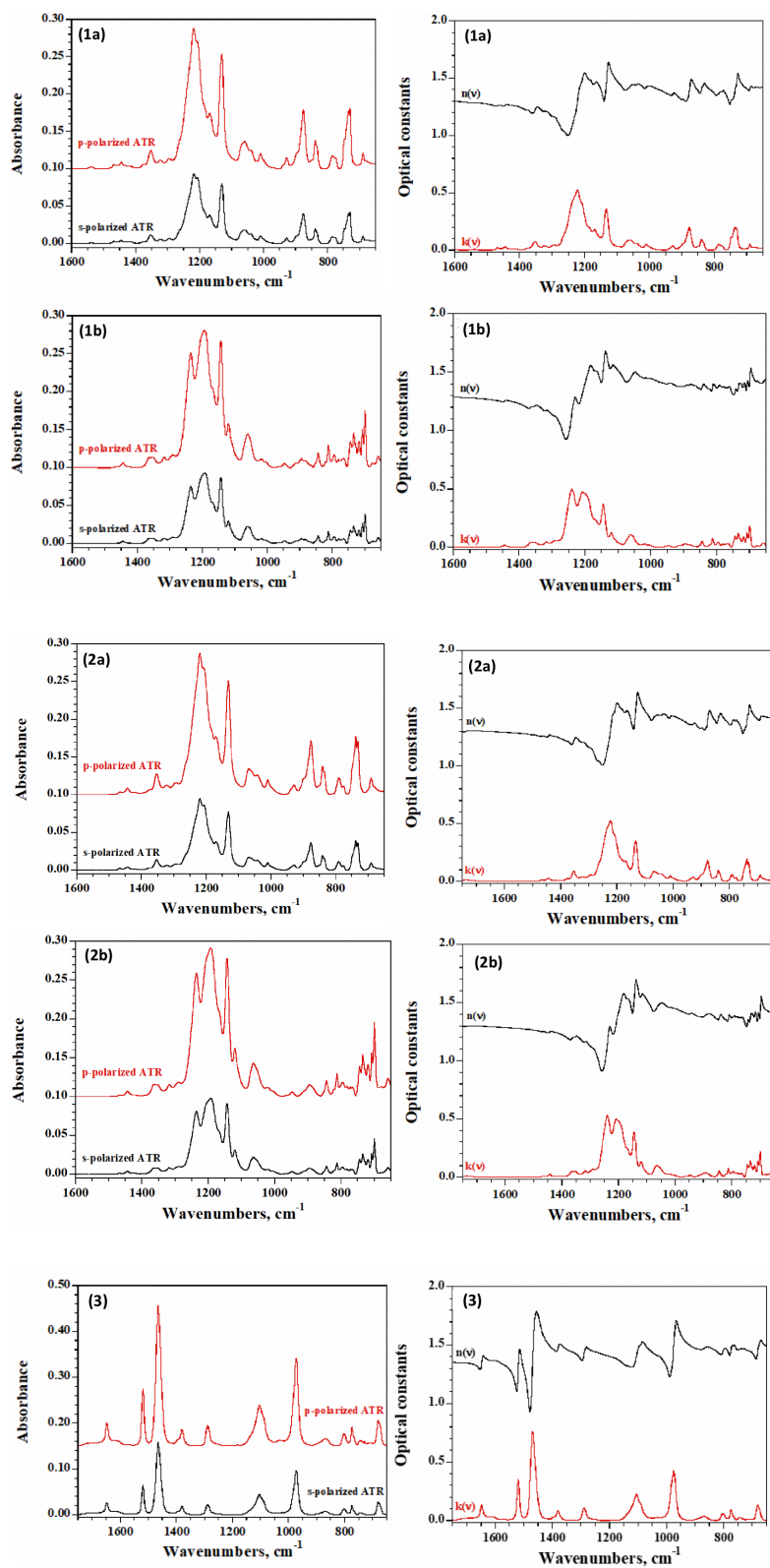


Figure S35. *p*- and *s*-polarized ATR spectra and isotropic optical constants of **1a**, **1b**, **2a**, **2b** and **3**.

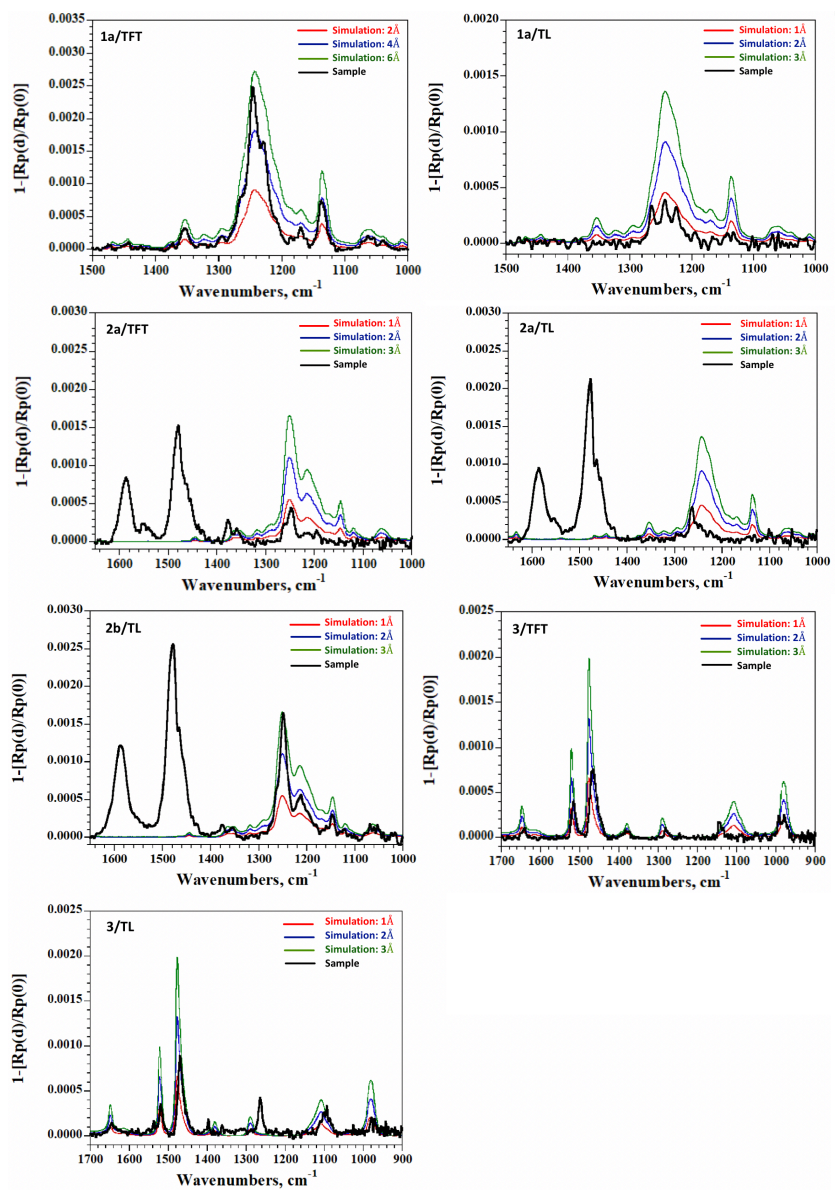


Figure S36. PM-IRRAS spectrum of different modified perovskite surfaces (black lines). Simulated spectra of compact isotropic layer with different thicknesses (colored lines).

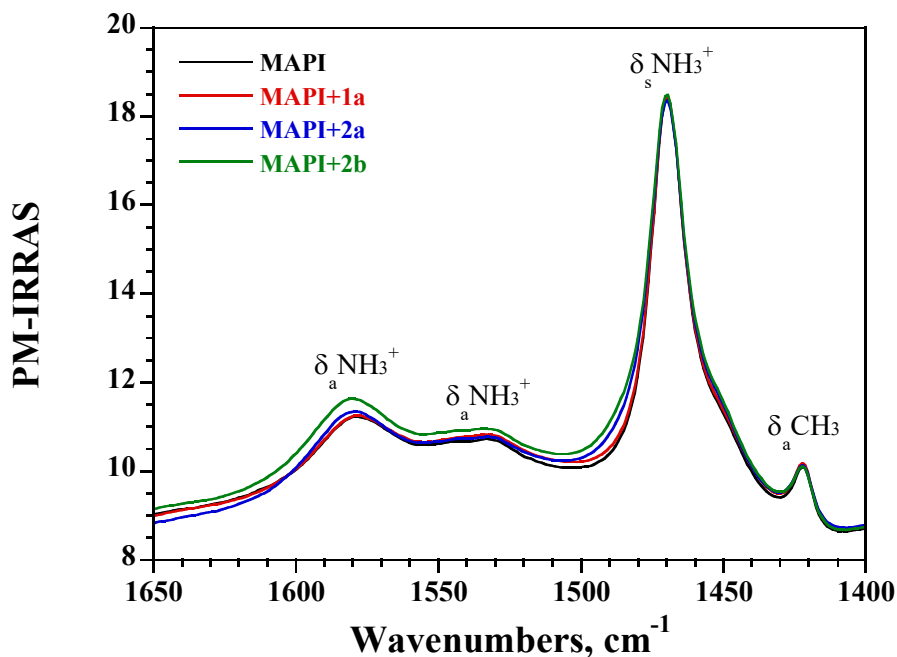


Figure S37. Overlay of the PM-IRRAS spectrum of different modified perovskite surfaces showing the broadening of the symmetric and antisymmetric bending vibrations of the NH_3^+ group resulting from the presence of **2**.

REFERENCES

- (1) Y. Imakura, S. Nishiguchi, A. Orita, J. Otera, Assessment of Fluoroalkyltin Compounds as Fluorous Lewis Acid Catalysts. *Appl. Organomet. Chem.* **2003**, *17*, 795–799.
- (2) D. P. Curran,; M. Hoshino, Stille Couplings with Fluorous Tin Reactants: Attractive Features for Preparative Organic Synthesis and Liquid-Phase Combinatorial Synthesis. *J. Org. Chem.* **1996**, *61*, 6480–6481.
- (3) M. J. Dignam, S. Mamiche-Afara, Determination of the Spectra of the Optical Constants of Bulk Phases via Fourier Transform ATR. *Spectrochim. Acta A Mol.spectrosc.* **1988**, *44*, 1435–1442.
- (4) W. N. Hansen, Electric Fields Produced by the Propagation of Plane Coherent Electromagnetic Radiation in a Stratified Medium. *J. Opt. Soc. Am.* **1968**, *58*, 380–390.
- (5) T. Buffeteau, B. Desbat, Thin-Film Optical Constants Determined from Infrared Reflectance and Transmittance Measurements. *Appl. Spectrosc.* **1989**, *43*, 1027–1032.
- (6) K. Yamamoto, H. Ishida, Interpretation of Reflection and Transmission Spectra for Thin Films: Reflection. *Appl. Spectrosc.* **1994**, *48*, 775–787.
- (7) E. D. Palik, *Handbook of Optical Constants of Solids*; Academic Press, 1998.